SCIENTIFIC REPORTS

OPEN

SUBJECT AREAS:
BIOLOGICAL FLUORESCENCE
BIOPHYSICAL CHEMISTRY
PROTEINS
PHOTOCHEMISTRY

Received
18 December 2012

Accepted
7 March 2013

Published
3 April 2013

Correspondence and requests for materials should be addressed to S.K.P. (skpal@bose.res.in) or S.M. (mayor@ncbs.res.in)

* These authors contributed equally to this work.

Light driven ultrafast electron transfer in oxidative redding of Green Fluorescent Proteins

Ranajay Saha[1]*, Pramod Kumar Verma[1]*, Surajit Rakshit[1], Suvrajit Saha[2], Satyajit Mayor[2] & Samir Kumar Pal[1]

[1]Unit for Nano Science & Technology, Department of Chemical, Biological & Macromolecular Sciences, S. N. Bose National Centre for Basic Sciences, Block JD, Sector III, Salt Lake, Kolkata 700098, India, [2]National Centre for Biological Science (TIFR), Bellary Road, Bangalore 560 065, India.

Fluorescent proteins undergoing green to red (G/R) photoconversion have proved to be potential tools for investigating dynamic processes in living cells and for photo-localization nanoscopy. However, the photochemical reaction during light induced G/R photoconversion of fluorescent proteins remains unclear. Here we report the direct observation of ultrafast time-resolved electron transfer (ET) during the photoexcitation of the fluorescent proteins EGFP and mEos2 in presence of electron acceptor, p-benzoquinone (BQ). Our results show that in the excited state, the neutral EGFP chromophore accepts electrons from an anionic electron donor, Glu222, and G/R photoconversion is facilitated by ET to nearby electron acceptors. By contrast, mEos2 fails to produce the red emitting state in the presence of BQ; ET depletes the excited state configuration en route to the red-emitting fluorophore. These results show that ultrafast ET plays a pivotal role in multiple photoconversion mechanisms and provide a method to modulate the G/R photoconversion process.

In the last few decades green fluorescent protein (GFP) and its variants have revolutionized our ability to visualize the key molecular processes occurring in live cells and many other research fields[1]. Recently a new class of photoconvertible fluorescent proteins has been developed whose emission properties can be changed upon illumination of light at specific wavelengths[2–5]. For example, GFP[6], Kaede[7], and EosFP[8] convert irreversibly from green to red (G/R) on irradiation by UV or violet light. This spectral shift caused by irradiation allows the investigation of dynamics in live cells or designing super resolution imaging schemes based on photoactivated localization microscopy[9,10]. Despite the obvious value of photoconversion of fluorescent proteins, key photo-excited processes such as electron transfer (ET) and proton transfer that underlie significant spectral changes in the chromophore, have remained poorly understood.

Green fluorescent protein (GFP) from jellyfish *Aequorea victoria* absorbs predominantly at 398 nm. Irradiation with blue light irreversibly transforms this state to red fluorescence state with corresponding excitation-emission maxima at 525 and 600 nm, respectively[6]. The term 'redding' is used to describe this photoconversion[11]. The red form of the protein is stable in anaerobic condition, but it disappears after re-oxygenation of the sample[6]. Recently very efficient green to red photoconversion in enhanced GFP (EGFP) was observed upon irradiation with at 488 nm in presence of various electron acceptors including p-benzoquinone (BQ), implicating ET in G/R photoconversion of EGFP and other fluorescent proteins (FPs)[11]. However, an understanding of the role of ET and allied processes (proton transfer) can only be obtained from studying the time-resolved dynamics of the excited states of G/R photoconvertible fluorescent proteins (PCFPs). Here, using femtosecond up-conversion technique as well as picosecond-resolved fluorescence spectroscopy, we explore the ultrafast excited state dynamics of PCFPs. We find that while BQ promotes efficient G/R photconversion in EGFP, by contrast, BQ abolishes G/R photoconversion of mEos2; ultrafast fluorescence spectroscopy provides us clear evidence for the differing roles of ET in the excited states of these PCFPs.

Results

An ultrafast view of the photoconversion process in EGFP. Oxidative photoconversion of EGFP in presence of electron acceptor, BQ, leads to loss of typical EGFP fluorescence emission (compare Fig. 1a, curves 3 and 4),

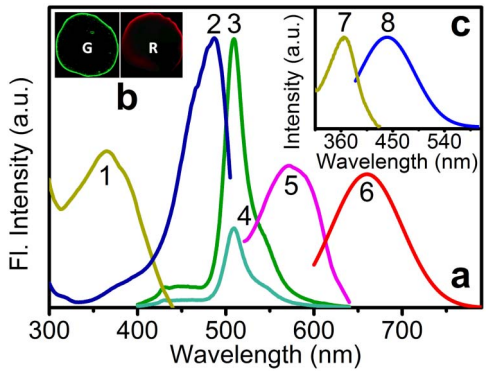

Figure 1 | Excitation-emission spectra of EGFP in presence and absence of BQ. (a) Excitation spectrum of EGFP monitored at 440 nm (1) and at 540 nm (2). Emission spectrum of EGFP excited at 375 nm in absence (3) and presence of BQ (4). Excitation spectrum of EGFP in presence of BQ monitored at 660 nm (5). Emission spectrum of EGFP in presence of BQ excited at 575 nm (6). (b) Fluorescence microscopic images of EGFP in absence of BQ excited at blue light (G) and in presence of BQ excited at green light (R). (c) Excitation spectrum of EGFP at pH 3.0 monitored at 440 nm (7). Emission spectrum of EGFP at pH 3.0 excited at 375 nm (8).

concomitant with the appearance of red photoconverted protein (Fig. 1b) with corresponding fluorescence excitation and emission maxima at 575 (Fig. 1a, 5) and 660 nm (Fig. 1a, 6), respectively.

To explore the mechanism of the photoconversion we observe time-resolved (both femtosecond and picosecond) dynamics of the electronic states of EGFP in absence and presence of BQ, using ultrafast spectroscopy. To understand the photochemical reactions taking place during this photoconversion reaction, it is important to appreciate that at neutral pH EGFP may exist in multiple ground states; a neutral (A state) and two deprotonated anionic states (B, and I), appear to dominate the landscape (Fig. 2). Indeed, the excitation spectrum of EGFP at neutral pH monitored at the emission wavelengths of 440 nm (A state) and 540 nm (B and I states) show evidence for these states (Fig. 1a, curves 1 and 2); the neutral chromophoric form (A state) has excitation maximum around ~365 nm, whereas the excitation maximum near ~488 nm can be attributed to the deprotonated anionic chromophores (B and I)[12,13]. Consistent with this, at acidic pH (pH 3.0) the A state is the predominant chromophore, giving a singular excitation and emission profiles with maxima at ~365 and ~440 nm, respectively (Fig. 1c, curves 7 and 8).

At neutral pH, in the excited state, the neutral chromophore A* depopulates mainly via an excited state proton transfer (ESPT) reaction to I*, which can evolve further to a more relaxed state B* (Fig. 2). ESPT reaction of EGFP has been studied in detail and occurs via a hydrogen-bond network comprising a water molecule and the side chain of Ser205, with subsequent protonation to the γ-carboxylate group of Glu222[14,15]. Consistent with this mechanism, using femtosecond fluorescence up-conversion technique when EGFP is excited at 390 nm, A* decays rapidly to form excited state species I* by ESPT due to deprotonation of the neutral chromophore, as seen by the rapid decay (3.51 and 20.13 ps) of blue emission characteristic of A* at 470 nm followed by the corresponding rise (2.12 and 18.39 ps) of the green emission at 510 nm (Fig. 3a and Table 1). At neutral pH, in presence of oxidant BQ, the femtosecond-resolved fluorescence transients characteristic of A* (at 470 nm) shows a major (73%) ultrafast time component of 220 fs in addition to the transients responsible for ESPT (3.40 and 13.46 ps) (Fig. 3a and Table 1). The appearance of the fs time component is unlikely due to any change in the overall structure and ground state property of the fluorophore in the protein, since both the CD and absorbance spectra are respectively unaltered in the presence of BQ (Supplementary Fig. S2). The 220 fs time component is a signature of ET between EGFP and BQ, and indicates that excited neutral chromophore (A*) depopulates mainly via ET process in the presence of BQ (see also Fig. 3c and Supplementary Text). Although such fast time scales may also be obtained by ultrafast excitation energy transfer (EET) from A* to BQ, this could be ruled out by monitoring the rate of non-radiative processes (k_{nr}) obtained by equation 1, as a function of BQ concentration. The rate constant k_{nr} exhibits a linear dependence on BQ (Fig. 3b), whereas non-radiative energy transfer (e.g., via a Förster's mechanism) would have non linear dependence on BQ concentration.

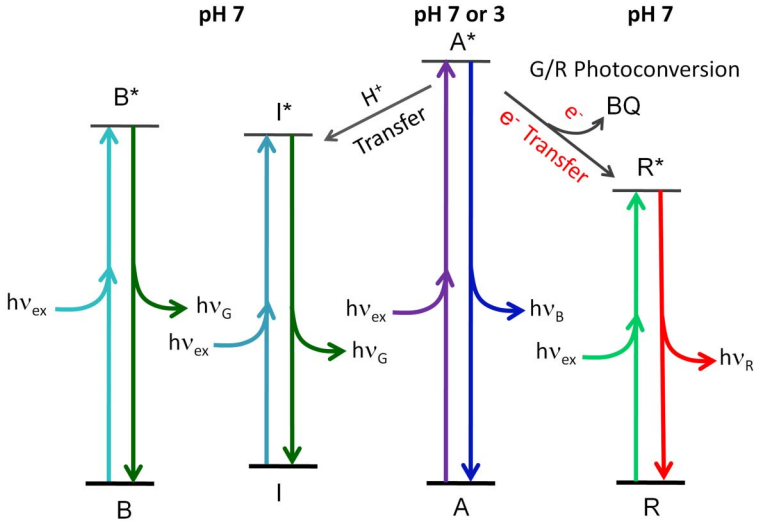

Figure 2 | Proposed electronic energy-level diagram of the various photoconvertable forms of EGFP. A, protonated form of the chromophore; I and B, deprotonated forms of the chromophore; R is the red photoconverted chromophore. A band excitation produces the excited state species A*, which can either decay giving blue emission or may undergo excited state proton transfer (ESPT) generating the anionic excited state chromophore I*. I* can either depopulate to ground state I giving green emission or may infrequently attain the more relaxed B* state with the chromophoric environment optimized for green emission. In presence of oxidant BQ, A* undergoes ultrafast electron transfer (ET) to generate the red emissive species R*. Both ET and excited state proton transfer (ESPT) are suppressed at lower pH (= 3) of the medium. The energy scheme for the A, B and I form is according to the reference[13]. The model is not accountable for the eventual processes between the ground state chromophoric forms of the protein.

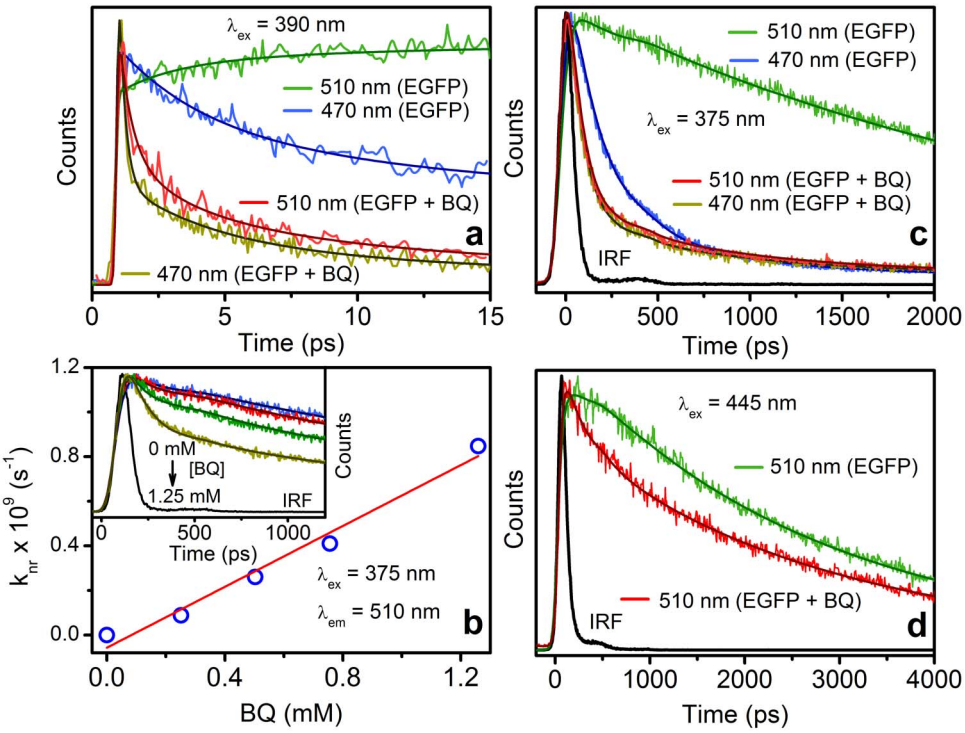

Figure 3 | Fluorescence decay transients of EGFP. (a) Femtosecond-resolved fluorescence decays of EGFP monitored at 470 and 510 nm (excitation wavelength 390 nm) in presence and absence of BQ. (b) Rate constants for nonradiative decay processes at various concentrations of BQ. The inset shows corresponding EGFP fluorescence decays monitored at 510 nm (excitation wavelength 375 nm). (c) Picosecond-resolved fluorescence decays of EGFP monitored at 470 and 510 nm (excitation wavelength 375 nm) in presence and absence of BQ (d) Picosecond-resolved fluorescence decays of EGFP monitored at 510 nm (excitation wavelength 445 nm) in presence and absence of BQ.

When, the detection wavelength is changed from 470 to 510 nm upon excitation of A band with 390 nm light the amplitude of the femtosecond transient decreases from 73% to 57% (Fig. 3a and Table 1) indicating that a fraction of A* is also transferred to I* through ESPT implying a competition between ET process and ESPT. Therefore, monitoring the sub-picosecond components of the rise and fall of fluorescence emission at 470 nm and 510 nm, respectively, provides characteristic information about A* and I* state dynamics. This underscores the use of an "all optical" femtosecond-resolved fluorescence detection system (up-conversion technique) for the exploration of relevant time components associated with ET dynamics (see Materials and Method).

As mentioned above, at neutral pH the EGFP ground state also consists of a deprotonated anionic chromophore, the B state. This may be preferentially excited with 445 nm diode laser (IRF ~80 ps) and its characteristic excited states detected by monitoring fluorescence emission decays at 510 nm (Fig. 3d). The detected fluorescence decay at 510 nm in presence of BQ is only slightly faster compared to that in its absence. This observation suggests that the anionic chromophore does not participate in ET. The reason for the

Table 1 | Fluorescence decay parameters of EGFP and mEos2 in presence and absence of BQ

	Excitation/nm	Emission/nm	a_1	τ_1/ps	a_2	τ_2/ps	a_3	τ_3/ps	a_4	τ_4/ps
EGFP	390[b]	470	0.40	3.51	0.20	20.13	0.40	132.46	-	-
		510	−0.09	2.12	−0.15	18.39	0.76	388.78	-	-
EGFP + BQ	390[b]	470	0.73	0.22	0.16	3.40	0.09	13.46	0.02	507
		510	0.57	0.22	0.30	3.40	0.08	13.00	0.05	285
EGFP	375[c]	470	0.42	31	0.46	198	0.09	578	0.03	4600
		510	−0.10	28	0.16	155	0.14	1469	0.80	3246
EGFP + BQ	375[c]	470	0.83	68	0.12	398	0.05	3363	-	-
		510	0.83	65	0.12	496	0.05	3471	-	-
EGFP	445[c]	510	−0.15	35	0.10	178	0.55	2377	0.50	3286
EGFP + BQ		510	0.40	77	0.16	597	0.44	2976	-	-
mEos2	375[c]	520	0.12	240	0.42	1160	0.46	3450	-	-
		580	0.13	240	0.16	1100	0.71	4420	-	-
mEos2 + BQ	375[c]	520	0.72	60	0.17	240	0.07	1160	0.04	4900
		580	0.71	60	0.19	240	0.08	1160	0.02	4650

τ_i represents decay time constant and a_i is its relative contribution.
[b]experiments were conducted on the femtosecond setup.
[c]experiments were conducted on picosecond setup.

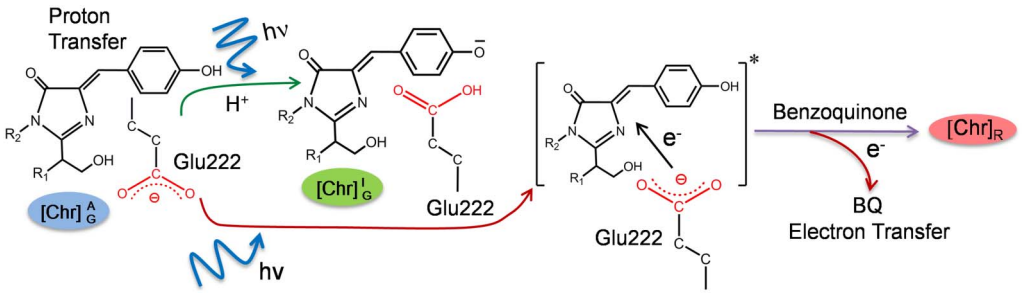

Figure 4 | Schematic of green to red photoconversion (G/R) of EGFP. Electron transfer during oxidative photoconversion of EGFP competes with the excited state proton transfer that initiates the dominant fluorescence photocycle. The ionized Glu222 is the key electron donor to the photoexcited chromophore prior to transfer of electron from the excited chromophore to the electron acceptor BQ. BQ favors G/R photoconversion in EGFP.

marginally faster decay kinetics is probably due to partial excitation of neutral chromophore 'A' by 445 nm laser pulse (see also Supplementary Text).

The anionic state of Glu222 facilitates excited state proton transfer in EGFP. In ESPT, the carboxylate side chain of Glu222 acts as the final proton acceptor[16], as proton transfer takes place from the neutral chromophore's tyrosyl hydroxyl group to the γ-carboxylate group of Glu222 via a hydrogen-bond network comprising water molecules and the side chain of Ser205, leading to the deprotonated anionic chromophore (I) from which green emission occurs[15]. At neutral pH, very efficient ESPT occurs as evident from the strong green emission (Fig. 1a, curve 3). However, at pH 4.2, the emission maximum is at ~450 nm (characteristic of neutral chromophore A) with a shoulder at ~510 nm (green emission) (Supplementary Fig. S1). Thus ESPT is significantly hindered at pH 4.2, and completely blocked at pH 3, with only blue emission is observed at this pH (Fig. 1c, curve 8).

This change in ESPT is not accompanied by any gross alteration in the secondary structure of EGFP, since CD measurements (Supplementary Fig. S2a) show that the secondary structure remains unperturbed with change in pH. Thus, the observed change in ESPT is likely to be a result of the modification of protonation state of Glu222. The internal proton-binding site in the γ-carboxylate group of Glu222 and the ionization equilibria of GFP-chromophore are mutually dependent. Two acid-base transitions of the chromophore occur at pH values 6.8 and 13.4[17]; at neutral and basic pH region, the local chromophore environment consists of a proton transfer relay to the bulk solvent through anionic Glu222 (strong proton acceptor) capable of efficient ESPT, resulting in green fluorescence from the anionic chromophore. At low pH, the state neutral Glu222 dominates, since the pK_a of the Glu side chain in solution is 4.07[18], providing a possible explanation for why Glu222 cannot act as a proton acceptor, resulting in a block of the ESPT pathway at pH 3. A similar explanation has been put forward for the blue emission from a GFP mutant (deGFP1) at low pH[19]. These results presented here also provide a strong rationale for the use of EGFP as a sensitive ratiometric pH sensor.

A central role for the anionic state of Glu222 in facilitating ET-dependent photoconversion in EGFP. Since the ESPT is blocked at acidic pH, we expected that the excited neutral chromophore A* would depopulate mainly through ET process. However, at pH 3 the decay transients measured at 450 nm in absence of BQ and its presence are almost similar (Supplementary Fig. S3), implying that EGFP also does not participate in ET with BQ at pH 3. Consequently, we do not observe any G/R photoconversion in presence of oxidant BQ at low pH. The study at low pH (pH 3) also shows that quenching of the fluorescence by BQ at 450 nm is almost completely suppressed (consistent with the proposed scheme). This observation also argues against ultrafast excitation energy transfer (EET) as a possibility of non-radiative energy transfer from A* to BQ on 390 nm excitation, since EET is expected to occur even at low pH.

The failure of photoconversion at low pH in the presence of oxidant BQ also indicates a role for the anionic state of Glu222. We propose that the excited state of the neutral protonated chromophore acts as an oxidant that will accept electron from the anionic Glu222 residue following which the excited state chromophore donates the electron to the electron acceptor BQ (Fig. 4). A detailed Stark spectroscopic investigation by Boxer and coworkers suggest that the imidazolidinone ring is certainly electron deficient in the excited state of the neutral, protonated chromophore[20]. Moreover, due to electronic excitation to higher energy states, the split HOMO and LUMO states are occupied by unpaired electrons[21]. In contrast to the ground state of the chromophore, where the molecular orbitals are occupied by paired electrons, the unpaired electron in the HOMO makes the excited state a better electron acceptor, and the lower ionization potential of the lone pair in the LUMO makes the excited state into a better donor. Thus, the excited state of a fluorophore is potentially a better electron acceptor as well as an electron donor. At neutral pH, Glu222 is ionized and thus facilitates the ET process. On the other hand, at pH 3, Glu222 becomes neutral (protonated) thereby unable to donate electron and hence ET is also shut off.

The role of ET in other PCFPs. Recent studies suggest that light induced electron donor capacity may be a common feature of many FPs, especially those that have a Tyrosine as a key amino acid in their chromophore[11]. Therefore we investigate the role of ET in a popular photoconvertible fluorescent proteins, mEos2 from the stony coral (*Lobophyllia hemprichii*) which also contains a Tyr in its fluorophore.

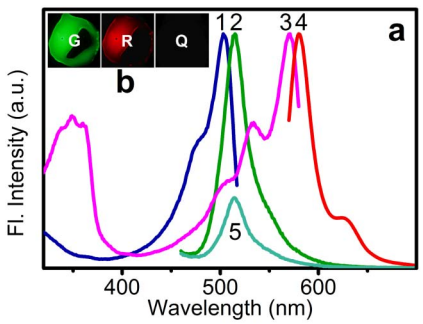

Figure 5 | Excitation-emission spectra of mEos2. (a) Excitation (1; monitored at 540 nm) and emission spectra (2; excited at 390 nm) of green form of mEos2. Excitation (3; monitored at 600 nm) and emission (4; excited at 560 nm) spectrum of red form of mEos2 obtained by irradiating mEos2 at 390 nm. Emission spectrum of mEos2 in presence of BQ (without irradiation) excited at 390 nm is marked 5. (b) Fluorescence microscopic images of mEos2 in absence of BQ excited at blue light (G) and green light (R) and in presence of BQ excited at green light (Q).

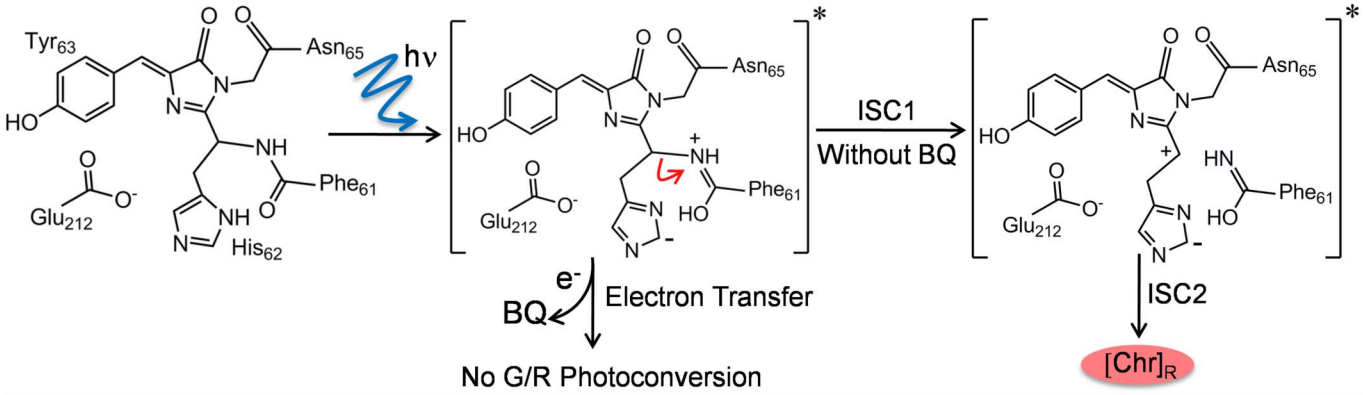

Figure 6 | Schematic of green to red photoconversion (G/R) of mEos2. Green to red (G/R) photoconversion of mEos2 in absence and presence of BQ. On irradiation, mEos2 undergoes two intersystem crossings (ISCs) to give the red form. However, BQ abolishes such a process by providing an alternative route for the de-excitation of the electron rich chromophore.

mEos2 shows highly efficient green emission (Fig. 5a, curve 2), when excited at 390 nm. The green form of mEos2 arises via autocatalytic maturation in the dark, yielding a cis-coplanar two ring chromophore chemically identical to that found in GFP. Irradiation with near-UV light at ~390 nm causes conversion of the green to the red emitting state (Fig. 5b)[8]. The red chromophore in mEos2, with excitation and emission maxima at 571 (with a vibronic sideband at 533 nm) and 580 nm (with a vibronic band at 630 nm), respectively (Fig. 5a, curves 3 and 4), is generated by cleavage of a peptide backbone. The break occurs between His-62 N_α-C_α bond (Fig. 6) with concomitant extension of the conjugated π electron system in the interior of the β-barrel without disruption of the tertiary structure[22].

To probe the role of ET in the G/R photoconversion of mEos2, we monitor the emission spectra of the protein treated with BQ. Notably, the fluorescence intensity of mEos2 is substantially quenched in presence of BQ (compare Fig. 5a, curves 2 and 5), however no prominent emission peak at 580 nm (red state) is generated even after prolonged irradiation (Supplementary Fig. S4). Significantly, while BQ has no effect on the ground state of the fluorophore (Supplementary Fig. S5), it rapidly photoconverts the excited state into a non-fluorescent species, preventing any further photo-excitation (Supplementary Fig. S4). To examine the time scale associated with the excited state quenching phenomenon, we measure picosecond-resolved fluorescence decay of BQ treated protein using 375 nm laser excitation. In absence of BQ, green and red states (Supplementary Fig. S6) of mEos2, have different decay parameters with average lifetimes ($<\tau> = \Sigma a_i\tau_i$) of 2.10 and 3.36 ns, respectively (Figs. 7a, b). However, fluorescence transients monitored at 520 nm and 580 nm, for BQ treated protein demonstrate similar decay characteristics (Table 1 and Fig. 7a and b) with a major ultrafast time component of 60 ps (Table 1), consistent with an ET process. The similarity in the decay behavior suggests that, in presence of BQ the emission measured at either wavelength arises predominantly from the same locally excited state species (i.e., green chromophore). Thus, BQ instead of promoting electron mediated G/R photoconversion like observed in EGFP shuts down the photoconversion in mEos2 showing essentially green emission with quenched decay times due to ET (Table 1). The observation clearly reveals the role of electron channeling via an alternate path thereby competing with photoconversion.

Recently, computer simulations have been used to understand the photoconversion pathway of mEos2 which involves excitation of the green protonated form to the S1 (singlet) state generating a transient imidazolide anion[23]. Subsequently, the system undergoes intersystem crossing to the triplet state, from which the peptide bond cleavage proceeds to form red emitting form[23]. It is to be noted that the ultrafast ET between mEos2 and BQ takes place on a time scale of 60 ps which is much faster than intersystem crossing of singlet excited state of chromophore to the triplet state, which is of the order of nanosecond[23]. Consequently, presence of electron acceptor (here BQ) provides the photoexcited mEos2 an alternate ultrafast deactivation pathway rather than undergoing slow intersystem crossing (Fig. 6), inhibiting G/R photoconversion.

Discussion

This ability of electron acceptor (here BQ) to control the G/R photoconversion in EGFP and EGFP like photoconvertible fluorescent proteins (mEos2, Kaede[7], DendFP[24], mcavRFP and rfloRFP[25])

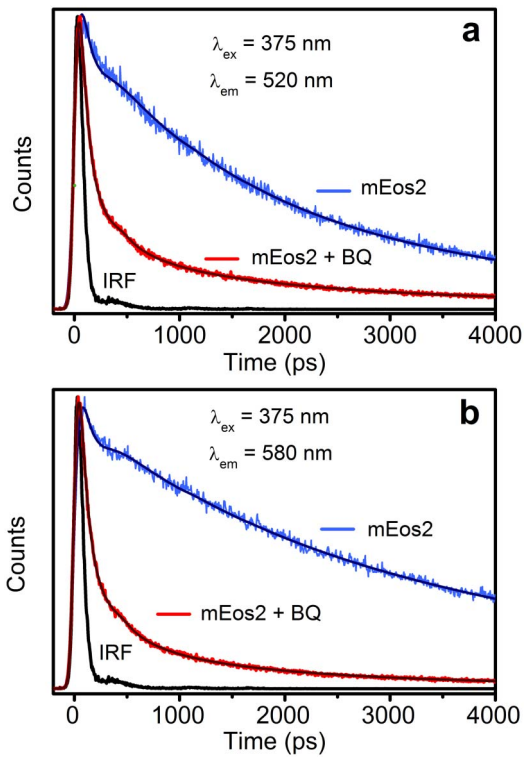

Figure 7 | Fluorescence decay transients of mEos2. (a) Picosecond-resolved fluorescence transients of mEos2 monitored at 520 nm in presence and absence of BQ (excitation wavelength 375 nm). (b) Picosecond-resolved fluorescence transients of mEos2 monitored at 580 nm in presence and absence of BQ (excitation wavelength 375 nm) (Solid lines are best fit to the experimental data).

suggests the central role of ET in red chromophore formation in PCFP. In summary, the present work shows an active role of light triggered ET in G/R photoconversion. This strengthens the legitimate use of the photoconversion of EGFP as detectors of electron acceptors as suggested earlier[11]. However, light-induced electron donors can affect the redox balance in the cell by providing reducing equivalents upon photo-excitation, and this may account for some of the photo-toxicity of the fluorescent proteins[26]. For the mEos2 protein, although it has a similar ground state chromophore (Fig. 6), our experiments suggest that ET causes a depletion of the chromophore itself by channeling the reaction in the excited state towards a different fate, effectively competing with the photoconversion process. This raises a cautionary note about using mEos2 proteins to quantitatively detect intracellular protein distribution and dynamics. The presence of high concentration of electron acceptors in areas such as the mitochondrion, will cause a rapid photochemical conversion of the excited states of these proteins, rendering them of limited applicability. Finally, the femtosecond/picosecond-resolved fluorescent transients presented here provide evidence for the ultrafast time scales associated with ET during the photoconversion process, that unequivocally implicate ET in sculpting spectral changes in emission wavelengths and photochemical changes upon irradiation.

Methods

Sodium dihydrogen phosphate, di-sodium hydrogen phosphate, sodium acetate and acetic acid were purchased from Sigma. p-Benzoquinone (BQ) was from Alfa Aesar. Protein solutions were prepared in either phosphate buffer solution (10 mM, pH 7.0) or sodium acetate buffer solution (10 mM, pH 3.0 and pH 4.2). For picosecond measurements we used 0.5 μM EGFP and 2 mM BQ solutions. To get sufficient photon count in femtosecond up-conversion measurements we used 14.5 μM EGFP, with concentration of BQ being 57 mM. In picosecond-resolved studies of mEos2 (0.67 μM) the concentration of BQ was 2.6 mM.

EGFP was obtained from MC4100 Escherichia coli (*E. coli)* cells containing pEGFP (Clontech), as described earlier[27]. The plasmid pRSETA harboring mEos2 was transformed into *E. coli* BL21DE3 cells and mEos2 was obtained from the protein purification facility at the Centre for Cellular and Molecular Platforms (C-CAMP, Bangalore, India).

Steady-state emission spectra were measured with a Jobin Yvon Fluoromax-3 fluorimeter. Fluorescence transients were measured using commercially available spectrophotometer (LifeSpec-ps) from Edinburgh Instrument, U.K. (excitation wavelength 375, and 445 nm, 80 ps instrument response function (IRF)) and fitted using FAST software provided by Edinburgh Instrument. Briefly, the observed fluorescence decay transients were fitted by using a nonlinear least square fitting procedure to a function $\left(X(t) = \int_0^t E(t')R(t-t')dt'\right)$ comprising of convolution of the IRF (E(t)) with a sum of exponentials $\left(R(t) = A + \sum_{i=1}^{N} B_i e^{-t/\tau_i}\right)$ with pre-exponential factors (B_i), characteristic lifetimes (τ_i) and a background (A). Relative concentration in a multi-exponential decay is finally expressed as; $a_n = \frac{B_n}{\sum_{i=1}^{N} B_i}$. The quality of the curve fitting is evaluated by reduced chi-square and residual data.

The femtosecond-resolved fluorescence were measured using a femtosecond up-conversion setup (FOG 100, CDP). The samples were excited at 390 nm (0.5 nJ per pulse), using the second harmonic of a mode-locked Ti-sapphire laser with an 80 MHz repetition rate (Tsunami, Spectra Physics), pumped by 10 W Millennia (Spectra Physics). The fundamental beam was frequency doubled in a nonlinear crystal (1 mm BBO, $q = 25^\circ$, $f = 90^\circ$). Using a gate pulse of the fundamental beam, the fluorescence emitted from the sample was up-converted in a nonlinear crystal (0.5 mm BBO, $\theta = 10^\circ$, $\varphi = 90^\circ$). The upconverted light was dispersed in a double monochromator and detected using photon counting electronics. The instrument response time was determined from the cross-correlation function due to sum frequency generation between gate and excitation pulses. The cross-correlation function was obtained using the Raman scattering from water, displaying a full width at half maximum of approximately (FWHM) of 165 fs. The observed femtosecond resolved decays were fitted using a Gaussian shape for the exciting pulse.

The rate constants (k_{nr}) for nonradiative decay processes were determined by comparing the average lifetime of EGFP chromophore in absence ($<\tau_D>$) and presence ($<\tau_{DA}>$) of acceptor BQ, using the equation 1.

$$k_{nr} = \frac{1}{<\tau_{DA}>} - \frac{1}{<\tau_D>} \quad (1)$$

Circular dichroism (CD) measurements were carried out on a JASCO 815 spectropolarimeter. The scan speed of the measurements was 50 nm min^{-1} and each spectrum was the average of five scans. The spectral data were acquired over the range of 200–300 nm using a 0.5 cm path length cuvette with EGFP concentration of 1 μM. The CD signal of the buffer solutions were subtracted from the sample solution to get the sample spectra.

1. Tsien, R. Y. The green fluorescence protein. *Annu. Rev. Biochem.* **67**, 509–544 (1998).
2. Lukyanov, K. A., Chudakov, D. M., Lukyanov, S. & Verkhusha, V. V. Photoactivatable fluorescent proteins. *Nat. Rev. Mol. Cell Biol.* **6**, 885–890 (2005).
3. Ando, R., Mizuno, H. & Miyawaki, A. Regulated fast nucleocytoplasmic shuttling observed by reversible protein highlighting. *Science* **306**, 1370–1373 (2004).
4. Andresen, M. *et al.* Structure and mechanism of the reversible photoswitch of a fluorescent protein. *Proc. Natl. Acad. Sci. U. S. A.* **102**, 13070–13074 (2005).
5. Patterson, G. H. & Lippincott-Schwartz, J. A photoactivatable GFP for selective photolabeling of proteins and cells. *Science* **297**, 1873–1877 (2002).
6. Elowitz, M. B., Surette, M. G., Wolf, P. E., Stock, J. & Leibler, S. Photoactivation turns green fluorescent protein red. *Curr. Biol.* **7**, 809–812 (1997).
7. Ando, R., Hama, H., Yamamoto-Hino, M., Mizuno, H. & Miyawaki, A. An optical marker based on the UV-induced green-to-red photoconversion of a fluorescent protein. *Proc. Natl. Acad. Sci. U. S. A.* **99**, 12651–12656 (2002).
8. McKinney, S. A., Murphy, C. S., Hazelwood, K. L., Davidson, M. W. & Looger, L. L. A bright and photostable photoconvertible fluorescent protein. *Nat. Methods* **6**, 131–133 (2009).
9. Betzig, E. *et al.* Imaging intracellular fluorescent proteins at nanometer resolution. *Science* **313**, 1642–1645 (2006).
10. Wiedenmann, J. & Nienhaus, G. U. Live-cell imaging with EosFP and other photoactivatable marker proteins of the GFP family. *Expert Rev. Proteomics* **3**, 361–374 (2006).
11. Bogdanov, A. M. *et al.* Green fluorescent proteins are light-induced electron donors. *Nat. Chem. Biol.* **5**, 459–461 (2009).
12. Chattoraj, M., King, B. A., Bublitz, G. U. & Boxer, S. G. Ultra-fast excited state dynamics in green fluorescent protein: multiple states and proton transfer. *Proc. Natl. Acad. Sci. U. S. A.* **93**, 8362–8367 (1996).
13. Creemers, T. M. H., Lock, A. J., Subramaniam, V., Jovin, T. M. & Volker, S. Three photoconvertible forms of green fluorescent protein identified by spectral hole-burning. *Nat. Struct. Mol. Biol.* **6**, 557–560 (1999).
14. Brejc, K. *et al.* Structural basis for dual excitation and photoisomerization of the Aequorea victoria green fluorescent protein. *Proc. Natl. Acad. Sci. U. S. A.* **94**, 2306–2311 (1997).
15. Stoner-Ma, D. *et al.* Observation of excited-state proton transfer in green fluorescent protein using ultrafast vibrational spectroscopy. *J. Am. Chem. Soc.* **127**, 2864–2865 (2005).
16. Jung, G., Wiehler, J. & Zumbusch, A. The photophysics of green fluorescent protein: influence of the key amino acids at positions 65, 203, and 222. *Biophys. J.* **88**, 1932–1947 (2005).
17. Scharnagl, C., Raupp-Kossmann, R. & Fischer, S. F. Molecular basis for pH sensitivity and proton transfer in green fluorescent protein: protonation and conformational substates from electrostatic calculations. *Biophys. J.* **77**, 1839–1857 (1999).
18. Voet, D. & Voet, J. G. *Biochemistry*, (J. Wiley & Sons, 2004).
19. Hanson, G. T. *et al.* Green fluorescent protein variants as ratiometric dual emission pH sensors. 1. structural characterization and preliminary application. *Biochemistry* **41**, 15477–15488 (2002).
20. Bublitz, G., King, B. A. & Boxer, S. G. Electronic structure of the chromophore in green fluorescent protein (GFP). *J. Am. Chem. Soc.* **120**, 9370–9371 (1998).
21. Klessinger, M. & Michl, J. *Excited states and photochemistry of organic molecules* (VCH, 1995).
22. Mizuno, H. *et al.* Photo-induced peptide cleavage in the green-to-red conversion of a fluorescent protein. *Mol. Cell* **12**, 1051–1058 (2003).
23. Lelimousin, M., Adam, V., Nienhaus, G. U., Bourgeois, D. & Field, M. J. Photoconversion of the fluorescent protein EosFP: a hybrid potential simulation study reveals intersystem crossings. *J. Am. Chem. Soc.* **131**, 16814–16823 (2009).
24. Pakhomov, A. A., Martynova, N. Y., Gurskaya, N. G., Balashova, T. A. & Martynov, V. I. Photoconversion of the chromophore of a fluorescent protein from Dendronephthya sp. *Biochemistry (Moscow)* **69**, 901–908 (2004).
25. Shagin, D. A. *et al.* GFP-like proteins as ubiquitous metazoan superfamily: evolution of functional features and structural complexity. *Mol. Biol. Evol.* **21**, 841–850 (2004).
26. Carpentier, P., Violot, S., Blanchoin, L. & Bourgeois, D. Structural basis for the phototoxicity of the fluorescent protein KillerRed. *FEBS Lett.* **583**, 2839–2842 (2009).
27. Saxena, A. M., Udgaonkar, J. B. & Krishnamoorthy, G. Protein dynamics control proton transfer from bulk solvent to protein interior: a case study with a green fluorescent protein. *Protein Sci.* **14**, 1787–1799 (2005).

Acknowledgments

P.K.V. and S.R. thank CSIR (India) for research fellowships. We thank J. Udgaonkar for providing purified EGFP, and M. Neerathilingam (CCAMP, Bangalore) for purified mEos2, DST (India) for grants support, SR/SO/BB-15/2007 (SKP) and JC Bose fellowship (SM).

Author contributions

R.S., P.K.V., S.R., S.S., S.M. and S.K.P. designed the experiments. R.S., P.K.V. and S.R. performed the spectroscopic experiments. R.S., P.K.V., S.M. and S.K.P. conceived the experiments and wrote the paper.

Additional information

Supplementary information accompanies this paper at http://www.nature.com/scientificreports

Competing financial interests: The authors declare no competing financial interests.

How to cite this article: Saha, R. *et al.* Light driven ultrafast electron transfer in oxidative redding of Green Fluorescent Proteins. *Sci. Rep.* **3**, 1580; DOI:10.1038/srep01580 (2013).